J. Fluid Mech. (1993), *vol.* 255, *pp.* 103–127

The flow of ordered and random suspensions of two-dimensional drops in a channel

By HUA ZHOU AND C. POZRIKIDIS

Department of Applied Mechanics and Engineering Sciences, University of California at San Diego, La Jolla, CA 92093–0411, USA

(Received 25 September 1992 and in revised form 5 April 1993)

The flow of a periodic suspension of two-dimensional viscous drops in a closed channel that is bounded by two parallel plane walls executing relative motion is studied numerically using the method of interfacial dynamics. Ordered suspensions where at the initial instant the drops are arranged in several layers on a hexagonal lattice are considered for a variety of physical conditions and geometrical configurations. It is found that there exists a critical capillary number below which the suspensions exhibit stable periodic motion, and above which the drops elongate and tend to coalesce, altering the topology of the initial configuration. At sufficiently large volume fractions, a minimum drop capillary number exists below which periodic motion is suppressed owing to the inability of the drops to deform and bypass other neighbouring drops in adjacent layers. This feature distinguishes the motion of dense emulsions from that of foam. The effects of capillary number, viscosity ratio, volume fraction of the dispersed phase, lattice geometry, and instantaneous drop shape, on the effective stress tensor of the suspension are illustrated and the results are discussed with reference to theories of foam. Two simulations of a random suspension with 12 drops per periodic cell are performed, and the salient features of the motion are identified and discussed. These include pairing, tripling, and higher-order interactions among intercepting drops, cluster formation and destruction, and drop migrations away from the walls. The macroscopic features of the flow of random suspensions are shown to be significantly different from those of ordered suspensions and quite independent of the initial condition. The general behaviour of suspensions of liquid drops is compared to that of suspensions of rigid spherical particles, and some differences are discussed.

1. Introduction

Suspensions of deformable particles, including gas bubbles, liquid drops, capsules, and biological cells, exhibit a variety of behaviour and a broad spectrum of rheological properties. Their rich phenomenology is attributed to changes in the shape and orientation of the suspended particles under the influence of an external flow, as well as to interparticle and particle–wall interactions that may lead to particle clustering and enhanced migration away from the boundaries of the flow. The behaviour of a suspension in a particular domain of flow depends on a number of parameters including the volume fraction, initial spatial and size particle distribution, physical properties of the dispersed and suspending fluids, and the structural constitution and associated mechanical properties of the interfaces.

The rheology of suspensions of liquid drops with constant surface tension has been analysed on a number of occasions, and a series of studies has been devoted to illustrating the motion of dilute suspensions where particle interactions are neglected.

These asymptotic theories furnish macroscopic constitutive equations that incorporate the first-order contribution of the particles to the effective stress tensor of the suspension with respect to the particle volume fraction. Taylor (1932) considered suspensions of spherical liquid drops, Schowalter, Chaffey & Brenner (1968) and Frankel & Acrivos (1970) considered suspensions of slightly deformed liquid drops, and Kennedy, Pozrikidis & Skalak (1993) considered suspensions of highly deformed liquid drops in a simple shear flow.

Extending the first-order analyses to incorporate higher-order corrections is hampered by uncertainties in specifying the instantaneous spatial distribution of the particles. One effective, albeit artificial, way of bypassing this difficulty is to consider ordered suspensions in which the particles are arranged at the vertices of a lattice, and the external flow is such that the structure of the suspension is a periodic or an almost periodic function of time (Adler & Brenner 1985). Unfortunately, although ordered suspensions are known to form spontaneously under certain conditions, their occurrence is the exception rather than the rule, and there is sufficient evidence to indicate that their behaviour at moderate and large volume fractions is fundamentally different from that of random suspensions that are routinely encountered in practice. Several authors have presented detailed analyses of the motion of ordered suspensions where the particles are arranged on cubic and rectangular lattices, spanning the whole range from the dilute limit to maximum packing (Pozrikidis 1993). But in view of the above limitations, the results of these studies must be interpreted in a limited physical context.

Another group of studies has addressed the rheology of highly concentrated emulsions and foams (Bikerman 1973). A comprehensive review of relevant theoretical and experimental studies is given by Kraynik (1988), and more recent work is reported by Reinelt & Kraynik (1989, 1990) and Kraynik, Reinelt & Princen (1991). The bubbles or drops in a concentrated emulsion are separated by thin films of suspending fluid that meet at multiple junctions called the Plateau borders. In the absence of global motion, molecular forces or external agents are necessary in order to stabilize the films and to sustain the foam for an extended period of time. A typical rheological study of foam is based on a series of simplifications including two-dimensionality, monodisperse constitution, and perfectly periodic spatial structure. Bidisperse and polydisperse foams are considered by Khan & Armstrong (1987) and Kraynik *et al.* (1991) respectively. An effort to extend the theory to three dimensions has been made recently by Kraynik & Reinelt (1992) and Reinelt & Kraynik (1992).

A distinguishing feature of ordered foam motion considered in previous theoretical studies, is that the displacements of the centres of the thin films that separate cells are affine with respect to the macroscopic strain. As a result, the instantaneous structure and properties of the foam are determined exclusively by the instantaneous macroscopic strain, and the motion may be analysed merely on geometrical grounds neglecting the effects of fluid flow. Beginning with Princen (1979, 1983), a large number of studies have considered the elastic–plastic response at small capillary numbers. The flow within the films and at the Plateau borders is either overlooked (Princen 1979, 1983; Kraynik & Hansen 1986) or assumed to be independent of the global motion of the foam (Khan & Armstrong 1986, 1987; Kraynik & Hansen 1987). Since the dynamics is sustained mainly by capillary forces, these models are successful in predicting a yield-stress and an elastic behaviour, but have difficulties in assessing the viscous contribution in a rigorous manner and with reasonable confidence and sufficient accuracy.

In a recent study, Reinelt & Kraynik (1990) built on a previous analysis by Schwartz

& Princen (1987) to devise an improved foam model that is capable of accounting for the flow at the Plateau borders using a film withdrawal mechanism proposed by Mysels, Shinoda & Frankel (1959). This flow is considered to make the dominant contribution to the overall rate of viscous dissipation. The theoretical model is valid at small capillary numbers Ca based on the macroscopic strain and cell size, and pertains to circumstances where the interfaces in the thin-film region have become inextensible due to the presence of surfactants. In addition, the foam is assumed to be wet, which means that the volume fraction of the continuous phase is small enough that the suspension is highly concentrated, but large enough that the structure of the foam is a continuous function of the strain. The results of Reinelt & Kraynik (1990) showed that the foam is elastic for small but finite deformations, the effective viscosity increases as the volume fraction of the suspended phase is increased, and the viscous contribution to the instantaneous stress of the suspension scales with the capillary number raised to the $\frac{2}{3}$ power. More will be said about this model in §4 of this paper.

When the assumptions of extremely large volume fractions and ordered structure are relaxed, all available theoretical models become either ineffective or prohibitively complex and direct numerical simulation becomes necessary in order to make further progress. For suspensions of rigid spherical particles, the application of boundary integral and related methods has led to the successful tackling of a host of problems of long-standing interest. Brady and coworkers applied their Stokesian dynamics method to study the behaviour of monodisperse suspensions of spherical particles arranged in a monolayer in an infinite or bounded domain of flow (Brady & Bossis 1988; Durlofsky & Brady 1989; Nott & Brady 1991). More recently, Revay & Higdon (1992) applied this method to study the sedimentation of a suspension of monodisperse spheres of two different densities in a three-dimensional periodic arrangement.

For suspensions of deformable particles, the complications associated with non-spherical evolving shapes have presented unsurpassed obstacles to large-scale numerical simulation; previous studies of drop motions have been restricted to solitary or at best pairwise motions. As a compromise, one may reduce the dimensionality of the problem by considering the idealized case of two-dimensional suspensions with cylindrical interfaces (Zhou & Pozrikidis 1993, hereafter referred to as ZPI). There is no doubt that this removes a certain degree of physical relevance, as discussed in ZPI, but allows us to perform extensive numerical investigations. Overall, taking into account the complexity of the problem in its general form, the assumption of two-dimensional motion appears, at least to these authors, to be an acceptable simplification and a precursor of studying motions in three dimensions. Experimental observations have shown that non-dilute emulsions exhibit shear-thinning and elastic behaviour, where the latter is evidenced by a positive normal stress difference (Vadas, Goldsmith & Mason 1976; Han & King 1980). These features have been identified in ZPI for suspensions of a single array of drops, suggesting that two-dimensional models preserve some important aspects of three-dimensional emulsion flow.

Considering two-dimensional motions allows the application of the method of interfacial dynamics for performing large-scale dynamic simulations. This method is based on an improved version of the boundary integral method formulated by Rallison & Acrivos (1978) and developed further by Pozrikidis (1992). The numerical procedure involves computing the evolution of the interfaces by solving a system of Fredholm integral equations of the second kind for the interfacial velocity. The implementation of the method is described in ZPI. In the present paper, we shall apply this method to conduct extensive numerical investigations of the motion of suspensions with ordered and random structure. To this end, we re-emphasize the order-or-magnitude increase

in computational demands for the simulation of drops compared to that of rigid particles; for our most involved computations, the number of scalar unknowns is roughly 15 times that required for rigid spheres in a three-dimensional configuration, and 30 times that required for rigid cylinders or spheres arranged in a monolayer.

In ZPI we proposed a computational framework for studying the flow of suspensions of two-dimensional drops in channels. The physical model consists of a suspension of two-dimensional drops flowing in a channel which is bounded by two parallel plane walls. Considering wall-bounded instead of doubly periodic flows allows us to assess the effect of particle–wall interactions and circumvent computational difficulties associated with infinite divergent sums that are inherent in the two-dimensional double-periodic Green's function. In ZPI we studied the motion and stability of single files of drops with the main objectives being to examine the significance of drop size compared to the width of the channel, illustrate the effects of viscosity ratio and capillary number, and investigate the nature of the pairwise drop interactions.

In the present study we consider more involved configurations with a larger number of drops, assuming that the suspension is composed of an infinite sequence of periodic cells, and each cell contains several drops which either are arranged in a regular manner in several rows, or are dispersed in a random fashion. The numerical studies involve solving a series of initial value problems in which the motion of spatially periodic suspensions of drops is computed from a specific initial configuration. The parametric space explored in the numerical studies complements that considered by previous foam models corresponding to very large volume fractions and small capillary numbers. To this end, we remark that foam theories are based on the presence of intermolecular forces while our results are obtained by considering the fluid mechanics of the motion alone with a simple interfacial behaviour characterized by constant surface tension.

We perform dynamic simulations of ordered suspensions in an extended range of volume fractions, focusing, in particular, on the limit of high volume fractions where the suspension becomes concentrated and seemingly resembles a foam. These parametric studies address the effects of the viscosity ratio, capillary number, initial drop shape, and geometrical arrangement, and the results are discussed with reference to predictions of available models for foam. Furthermore, we perform two dynamic simulations of a random suspension that contains 12 drops within each periodic cell with different initial drop distributions. These simulations reveal a number of novel features concerning drop interactions and cluster formations and provide some insights into the effect of the initial conditions. The results allow us to assess the effect of the instantaneous particle shape and orientation on the effective properties of the suspension, and to identify salient differences in the behaviour of suspensions with random and ordered structure.

The behaviour of the suspended drops near the walls of the channel is an important aspect of the motion. Experimental observations have indicated that concentrated suspensions tend to slip over the boundaries of a channel with a slip velocity that depends upon the rate of the motion, the global structure of the suspension, and the smoothness of the wall; boundary effects are confined to the first adjacent layer of drops (Princen 1985; Kraynik 1988). Furthermore, experimental and theoretical studies have demonstrand that deformable particles migrate away from the boundaries of a flow (Smart & Leighton 1991; Kennedy *et al.* 1993), and the wall zone of a channel may be depleted of particles yielding a core–annular flow (Cox & Mason 1971; Gauthier, Goldsmith & Mason 1972; Vadas *et al.* 1976; Skalak, Özkaya & Skalak 1989). At high concentrations, the core moves in a plug-flow mode while the annular layer provides lubricating support. Our simulations of ordered suspensions will

illustrate the behaviour of interfaces near the walls of the channel. Our simulation of random suspensions will investigate collective drop migrations and the formation of particle-free zones.

Blanc *et al.* (1983) and Durlofsky & Brady (1989) found that dense suspensions of rigid spheres flowing between two parallel walls in a Couette flow device develop particle clusters, and the formation and destruction of clusters involve a variety of motions. At moderately high concentrations, the characteristic size of the clusters becomes comparable with the clearance of the channel. There is a critical concentration at which the suspension exhibits a singular behaviour similar to that observed in percolation-type processes. The hydrodynamic interactions between the clusters themselves and between the clusters and the boundaries cause increased rates of dissipation, and may force the suspension to engage in a plug-flow mode.

In the case of suspensions of liquid drops, the added factor of particle deformability and the feasibility of topological changes through particle coalescence provide relieving mechanisms that may prevent the onset of large stresses associated with particle interceptions and large cluster formations. The presence of intermolecular forces and surface-active agents will certainly play a crucial role in determining the nature of particle interactions in close contact. It is thus likely that a suspension of liquid drops will not exhibit a singular behaviour at the critical concentration, i.e. a percolation-like transition, at least at large enough capillary number and low enough drop viscosities. Evidence for this is provided by observations and measurements for concentrated emulsions and foams (Han & King 1980; Kraynik 1988), as well as by the numerical simulations reported in this paper.

In addition to eliminating large stresses, drop deformability is also responsible for an elastic–plastic behaviour of stable foams when the volume fraction exceeds the critical value corresponding to maximum packing of circular drops. The significance of drop size and concentration on the dynamics of the microstructure and the effective stresses of a dense emulsion are not understood with satisfactory accuracy, and some insights will be gained from the results of our studies.

Nott & Brady (1991) studied the effect of shear rate variations across a channel on the motion of a suspension of spherical particles due to an imposed pressure gradient, investigating, in particular, the consequences of particle migrations from regions of high shear rates to regions of low shear rates. A mean pressure gradient can be included in a straightforward fashion in our physical model, and will be considered in a forthcoming paper.

2. Problem statement and numerical method

We consider the motion of a periodic suspension of neutrally buoyant viscous drops with viscosity $\lambda\mu$ suspended in an ambient fluid with viscosity μ between two parallel plane walls in a relative translation, as shown in figure 1. We assume that there is no pressure drop in the axial direction other than that imposed by the restriction that the total flow rate along the channel is equal to zero. Physically, the channel is assumed to be closed at the two ends.

At small Reynolds numbers, the flow is governed by the equations of Stokes flow with the no-slip and no-penetration condition required over the two walls. Other boundary conditions are that the velocity and tangential component of the surface force are continuous across the interface of each drop, and the normal component of the surface force undergoes a discontinuity due to a constant surface tension γ.

We render all variables non-dimensional using as characteristic length the half-width

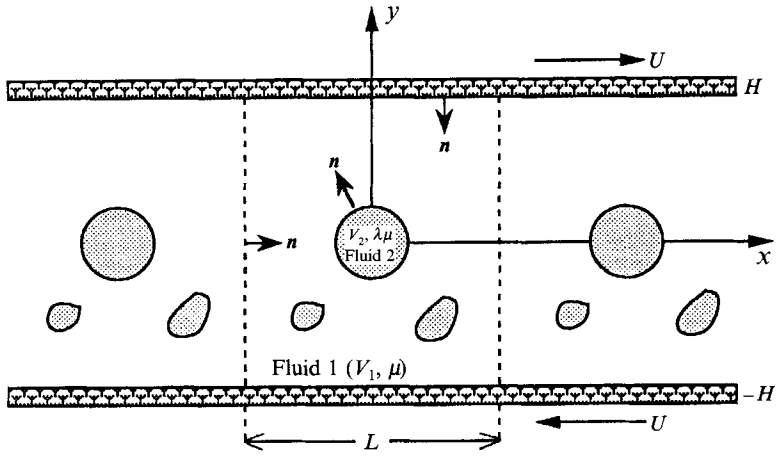

FIGURE 1. A periodic suspension of two-dimensional drops flowing in a channel. The motion is driven by the relative translation of the two walls; the channel is closed at both ends.

of the channel H, as characteristic velocity the wall velocity U, as characteristic time H/U, and as the characteristic stress $\mu U/H$. Assuming that all drops have identical areas we find that the motion depends on the viscosity ratio λ, capillary number $Ca = \mu U/\gamma$, and initial drop distribution. In certain parts of our discussion it will be appropriate to replace the macroscopic capillary number Ca with the drop capillary number $Ca_d = (a/H)\,Ca$ defined with respect to the equivalent radius of the drops a. The drop volume fraction ϕ_d is defined as the ratio of the total area of all drops contained in one periodic cell to the total area of the cell itself.

Using the boundary integral representation for Stokes flow, we express the velocity field in terms of the integral equations (1)–(2) presented in ZPI. Equation (2) of ZPI is a Fredholm integral equation of the second kind for the interfacial velocity whose solution may be computed by successive iterations. The rate of convergence of the iterations is increased by applying eigenvalue deflation. In the special case $\lambda = 1$, where the viscosity of the drops is equal to the viscosity of the suspending fluid, equation (2) of ZPI yields an expression for the interfacial velocity in terms of a contour integral over all interfaces.

The Green's function involved in the integral equation represents the flow due to an array of point forces along the channel. The associated pressure is adjusted so that the corresponding induced flow rate along the channel is equal to zero. This means that the pressure drop over one period of the flow is not equal to zero, but depends on the lateral position of the point forces. This Green's function is the natural choice for studying a flow with vanishing flow rate such as that established in a closed channel with moving walls. To study a flow with vanishing pressure drop, such as the flow established in a circular Couette flow device, it is appropriate to use a Green's function with an associated finite flow rate but vanishing pressure drop. This Green's function is derived from the previous one by adding an appropriate plane-Poiseuille flow.

Briefly, we compute the evolution of the suspension using the following procedure. First, we distribute a set of marker points along each drop interface, approximate the interface using cubic splines, and compute the normal vector and curvature by differentiating with respect to arclength. At the initial instant when the drop interfaces are circular, the marker points are evenly distributed along the interfaces. In the following time steps, the total number and density of marker points along each drop

interface is adjusted according to the local arclength and curvature (ZPI). Next, we solve the integral equation for the interfacial velocity field using an iterative method outlined in ZPI, and advance the position of the marker points using the Runge–Kutta–Fehlberg method of orders 2 and 3 (RKF23). The advantage of using an adaptive time-stepping scheme, such as the RKF23, over a fixed time-stepping scheme, such as a regular Runge–Kutta method, is that sawtooth-type numerical instabilities are eliminated by maintaining the numerical error under a specified threshold. For random suspensions, to minimize the CPU time, we use a simpler Euler's methods with a time step that is small enough that numerical instabilities are suppressed. Further details on the numerical procedure and accuracy of the computation are given in Zhou (1993).

To monitor the accuracy of the simulations, we compute the area of each drop at every time step. For drops initially arranged on a hexagonal lattice, the maximum change in area due to numerical error was less than 0.7% in all cases. For drops that are initially distributed in a random manner, the maximum change of the area could reach 1% after 40 time steps. To prevent the accumulation of this and related errors over the 620 steps of the simulation, we normalized the area of each drop after every 40 time steps by performing a weak isotropic expansion or compression. This artificial process has no fundamental effect on the behaviour of the suspension.

Almost all computations were performed on the CRAY Y-MP8/864 computer of the San Diego Supercomputer Center. For ordered suspensions, where the drops are arranged initially on a hexagonal lattice, a complete simulation typically required 30 min to 2 hr of CPU time. For each of the two random simulations with 12 drops per periodic cell and $\lambda = 1$, the computation required 6.5 CPU min for each time step at an approximate total expense of 67 CPU hr for about 620 time steps. Some simulations of two-layered suspensions were performed on SUN Sparcstations I.

3. Effective stresses and pressure drop

We define the effective stress tensor of the suspension $\langle \sigma_{ij} \rangle$ as the volume average of the stress tensor over the area of one periodic cell. It should be pointed out, however, that, because of the presence of the walls, the suspension is not homogeneous in all directions and the volume average $\langle \sigma_{ij} \rangle$ is not identical to the ensemble average, as it is for a homogeneous system (Batchelor 1970). But using the divergence theorem, one may show that $\langle \sigma_{12} \rangle$ is identical to the average shear stress over the walls of the channel, which has been defined by previous authors to be the effective shear stress of a suspension in shear-driven flow (Masliyah & van de Ven 1986; Durlofsky & Brady 1989). Furthermore, the present definition of the effective stress of the suspension may be justified on a rigorous basis by considering the behaviour of a general material whose boundary is subjected to a homogeneous strain (Goddard 1986).

In (11) of ZPI we derive an expression for $\langle \sigma_{ij} \rangle$ in the form

$$\langle \sigma_{ij} \rangle = -\delta_{ij}\langle P \rangle + 2\mu\langle e_{ij} \rangle + \frac{2}{A}\frac{\lambda - 1}{\lambda} E_{ij} + \frac{2}{A}\Sigma_{ij}, \tag{1}$$

where E_{ij} is the viscous stress tensor over the area of the drops given by

$$E_{ij} = \tfrac{1}{2}\mu\lambda \int_{S_D} (u_i n_j + u_j n_i)\, \mathrm{d}l \tag{2}$$

and Σ_{ij} is the surface-energy tensor given by

$$\Sigma_{ij} = \tfrac{1}{2}\gamma \int_{S_D} t_i t_j \, \mathrm{d}l. \tag{3}$$

The contour integrals are over all interfaces, $\boldsymbol{n}$ is the normal vector, and $\boldsymbol{t}$ is the tangent vector in the counterclockwise direction. It should be noted that (3) is a special case of the more general definition

$$\Sigma_{ij} = \gamma \int_{S_D} \kappa_m n_i x_j \, \mathrm{d}S = \tfrac{1}{2}\gamma \int_{S_D} (\delta_{ij} - n_i n_j) \, \mathrm{d}S \tag{4}$$

introduced by Rosenkilde (1967), which is applicable for closed three-dimensional interfaces; κ_m is the mean curvature. The second integral in (4) provides us with a convenient formula for computing the surface-energy tensor from the normal vector, circumventing the sensitive computation of the curvature. The viscometric functions include the effective shear viscosity μ_{EFF} and the normal stress difference $\mathcal{N}$. These are computed using equations (11)–(13) of ZPI.

When the viscosity of the drops is identical to that of the suspending fluid, i.e. $\lambda = 1$, non-isotropic effective stresses are due solely to surface tension, and $\langle \sigma_{ij} \rangle$ may be computed from knowledge of the instantaneous interfacial shape but not of the flow. In this case, $\langle \sigma_{ij} \rangle$ is identical to the average stress tensor computed by Reinelt & Kraynik (1989, 1990) for two-dimensional foam except that, in their case, the surface tension γ is a variable and must be placed inside the integral. It should be pointed out, however, that in the available theories of foam, the geometry of the drops is dictated by considerations that either ignore or account for a weak motion of the fluid.

In our simulations we require that the flow rate along the channel is equal to zero, which implies that the channel is closed at the ends. As a result, we obtain a finite pressure drop across each period of the cell, denoted by Δp. The parabolic flow associated with Δp is necessary in order to counteract the flow induced by drop motions and thus bring the total flow rate down to zero. For ordered suspensions with symmetric structure, the flow induced by drop motions vanishes and Δp is equal to zero, but for random suspensions Δp is finite, equal to the difference in the shear force exerted on the two walls. In our mathematical formulation, the pressure drop is mediated through a quadratic term in the Green's function shown in equations (A 11)–(A 12) of ZPI; clearly the value of Δp depends on the instantaneous drop profiles and spatial distribution.

4. Ordered suspensions

We consider the evolution of a periodic suspension of circular drops initially arranged on a hexagonal lattice, as illustrated in figure 2(*a*). When the volume fraction of the drops ϕ_a is less than the maximum volume fraction for touching circular drops ϕ_a^*, the drops may assume a circular hydrostatic shape that is required to minimize the total surface free energy of the mixture. Under the stipulation that the minimum separation between the drop surface and the wall is half the minimum separation between two neighbouring drops, we find that the initial state of the suspension is determined uniquely by specifying the number of rows N and the volume fraction ϕ_d. The drop radius a, the ratio of the minimum separation between two neighbouring drops D_{min} to the drop radius a, $\epsilon = D_{min}/a$, and periodicity L, may be com-

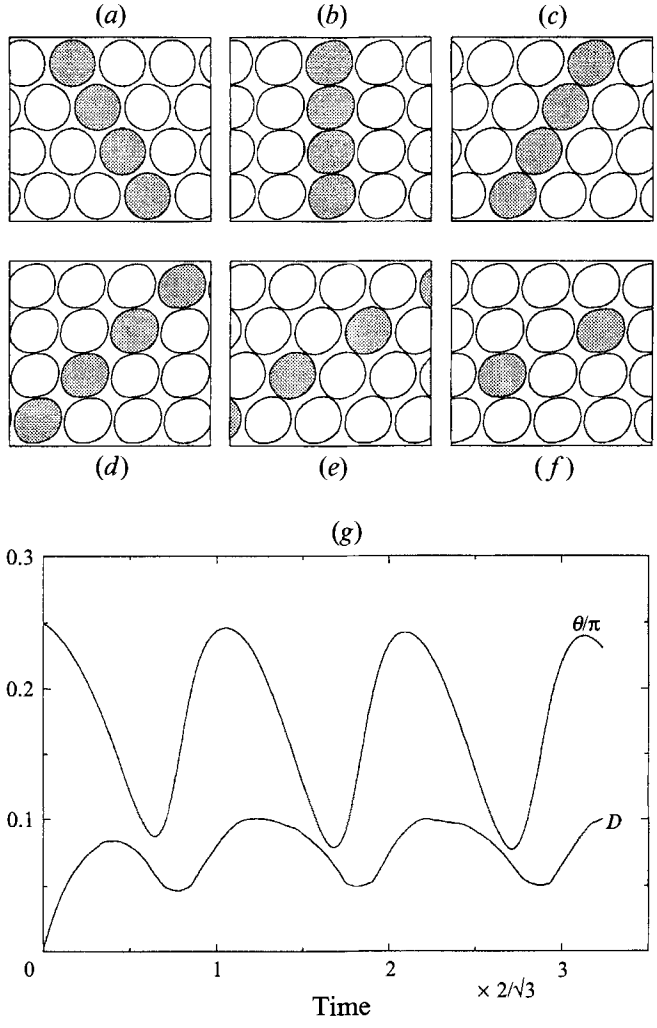

FIGURE 2. Drop profiles evolving from an initially hexagonal lattice of circular drops with four layers, for $\lambda = 1$, $Ca_d = 0.02527$, and $\phi_d = 0.7216$, at times: (*a*) $t = 0$, (*b*) $1/\sqrt{3}$, (*c*) $2/\sqrt{3}$, (*d*) $3/\sqrt{3}$, (*e*) $4/\sqrt{3}$, (*f*) $5/\sqrt{3}$; (*g*) the deformation parameter D and orientation angle θ.

puted using the geometrical conditions $\epsilon = -1 + [(\pi N/2\phi_d(2+\sqrt{3}(N-1)))]^{\frac{1}{2}}$, $a = 2/[(2+\sqrt{3}(N-1))(1+\epsilon)]$, and $L = 2(1+\epsilon)a$. The maximum volume fraction corresponding to touching drops is given by $\phi_d^* = N\pi/[2(2+\sqrt{3}(N-1))]$.

First, we consider motions for the computationally simplest case $\lambda = 1$. In ZPI we studied the motion of the single file, i.e. $N = 1$, and found that there exists a critical value of Ca below which the drops deform and obtain a stationary shape, and above which the drops continue to deform without ever reaching a steady state, independently of the drop size. In figure 2(*a*–*f*) we present a sequence of instantaneous drop profiles for $N = 4$, $Ca = 0.1$, or $Ca_d = 0.02527$, and $\phi_d = 0.7216$. Note that for $N = 4$ the maximum volume fraction for touching drops is $\phi_d^* = 0.87313$. The four shaded drops in the six frames may be used as a reference in order to monitor the relative motion of the individual layers in the evolving array.

Comparing the times corresponding to the six frames shown in figure 2(*a*–*f*) we find

that, after an initial transition period, the array evolves in a periodic manner with a period that is nearly equal to the time it takes each wall to travel one cell spacing downstream, i.e. $2/\sqrt{3}$. This indicates that the motion of the centres of the drops is approximately affine, meaning that the drops are convected nearly by the linear velocity field that would prevail in the absence of the drops, with a negligible slip velocity over the walls and negligible migration away from the walls. It is interesting to observe the switching of neighbouring drops and the coalescence and separation of the thin films at the Plateau borders, a process called 'hopping' by Prud'homme or 'T1' by Weaire (Kraynik 1988). We thus find that the basic micromechanical mechanism and some essential features of foam flow are captured in our simulations.

In figure 2(*g*) we present the corresponding evolution of the Taylor deformation parameter D of the drops in the second row, where $D = (L-M)/(L+M)$ and L, M are the maximum and minimum dimensions of a drop, and the drop orientation angle θ (Taylor 1934). It is clear that, after a short initial transition period, the drops deform in an oscillatory manner with a period that is almost identical to $2/\sqrt{3}$, and the amplitude of the oscillations is comparable with the corresponding mean values. The inclination of the drops varies from $\pi/4$ to almost $\pi/13$ through one cycle of the periodic motion. Minimum orientation corresponds to instants where drops in different layers lie over each other to form vertical columns. Furthermore, it is interesting to observe that there is a noticeable phase shift in the oscillations of D and θ. The rheological significance of this behaviour will be addressed later in our discussion. Our results for $Ca = 0.1964$, corresponding to $Ca_d = 0.04962$, reveal qualitatively similar drop profiles and behaviour.

In figure 3(*a–k*) we present a sequence of profiles for $Ca = 1.0$, corresponding to $Ca_d = 0.2527$, and observe that the drops assume a family of shapes that are hybrids of an elongated parallelogram and a slender elliptical shape. Close inspection reveals that the deformation and orientation of the drops that are adjacent to the walls are slightly different than those of the drops in the middle rows. Boundary effects are seen to cause a noticeable migration of the interfaces away from the walls, but have a small influence on the behaviour of the middle rows near the centreline of the channel. Evidently, the effect of the walls is shielded by the first adjacent layer of drops.

Diagrams of D and θ with respect to time for $Ca_d = 0.2527$, not shown in the text, revealed a monotonic increase with small oscillations around an asymptotic value, indicating that the motion of the suspension is not perfectly periodic. Inspecting figure 3(*g*, *i*, *k*) reveals that the thickness of the films that separate adjacent drops in each row diminishes in time, and the onset of dimpled interfacial shapes may be considered a precursor of film breakup and drop coalescence. Whether the drops will continue to elongate or coalesce at finite elongation, could not be assessed with confidence in our simulations. If the drops coalesce, the suspension will obtain a stratified layered structure, and the longitudinal velocity profile will be linear across each stratum.

Overall, our results indicate that a suspension with $Ca_d = 0.02527$ or 0.04962 executes stable periodic motion, whereas a suspension with $C_d = 0.2527$ is likely to suffer drop coalescence. It should be emphasized, however, that the presence of intermolecular forces and external agents will have a profound effect on the behaviour of the thin films, and might stabilize the suspension and sustain the periodic motion at high values of Ca_d. In general, our results are in agreement with experimental observations suggesting that a foam can be destroyed by subjecting it to a sufficiently high-shear-rate motion (Princen 1983).

Our results suggest the existence of a critical capillary number below which the drops execute a stable periodic motion and above which they continue to elongate and tend

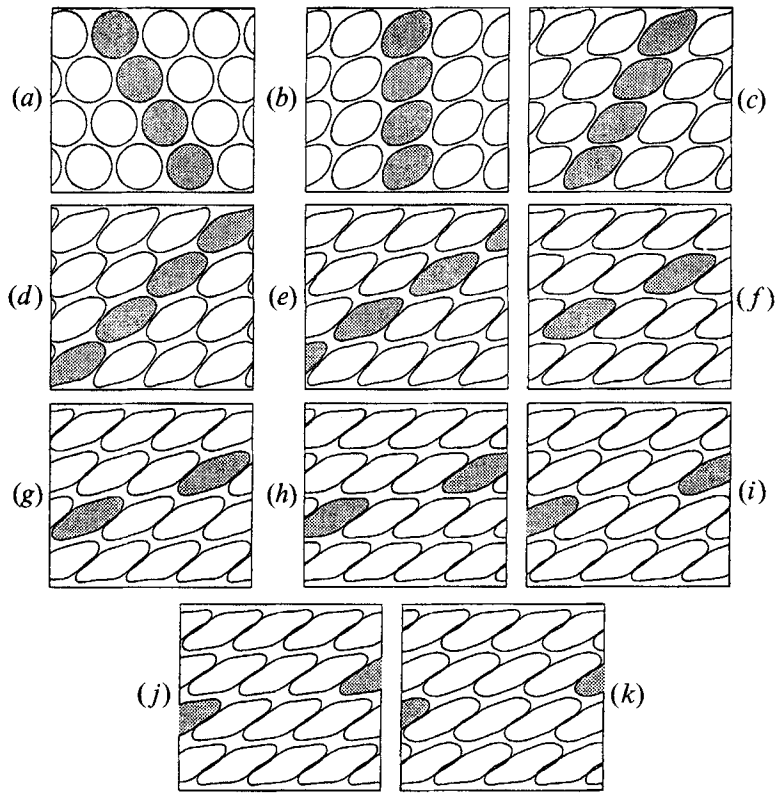

FIGURE 3. Drop profiles evolving from an initially hexagonal lattice of circular drops with four layers, for $\lambda = 1$, $Ca_d = 0.2527$, and $\phi_d = 0.7216$, at times: (*a*) $t = 0$, (*b*) $1/\sqrt{3}$, (*c*) $2/\sqrt{3}$, (*d*) $3/\sqrt{3}$, (*e*) $4/\sqrt{3}$, (*f*) $5/\sqrt{3}$, (*g*) $6/\sqrt{3}$, (*h*) $7/\sqrt{3}$, (*i*) $8/\sqrt{3}$, (*j*) $9/\sqrt{3}$, (*k*) $10/\sqrt{3}$. The effect of Ca_d may be assessed by comparing this figure with figure 2.

to coalesce altering the topology of the initial configuration. Stable motion, however, it not to be expected for small Ca_d at sufficiently large volume fractions $\phi_d > \phi_d^0$; here $\phi_d^0 = 3N\pi/[8(2+\sqrt{3}(N-1))]$ is the volume fraction when the vertical separation of the centres of drops at adjacent layers is equal to the drop diameter, i.e. $\epsilon = 2/\sqrt{3}-1$. Under these conditions the drops will resist deformation and will be unable to roll over each other in order to engage in a typical foam flow. Instead, they will press against each other instigating coalescence, while the walls will be slipping over the top and bottom rows. This behaviour was evident in our numerical simulations. In summary, at large volume fractions there exists a lower critical capillary number under the drops fail to execute the stable periodic motion described above.

4.1. *Effective stresses*

We consider next the behaviour of the effective stress tensor of the suspensions illustrated in figures 2 and 3. In figure 4(*a–c*), we plot the evolution of the effective shear viscosity μ_{EFF} and normal stress difference $\mathcal{N}$. Note that at the initial instant $\mu_{EFF} = 1$ because $\lambda = 1$, and $\mathcal{N} = 0$ because the drops have a circular, isotropic shape. Clearly, both μ_{EFF} and $\mathcal{N}$ exhibit oscillatory behaviour about well-defined mean values, and the amplitude of the oscillations decreases as Ca is increased, i.e. as the drops become more deformable. For $Ca_d = 0.02527$ the amplitudes of the oscillation are comparable with the corresponding mean values and the minimum value of $\mathcal{N}$ is

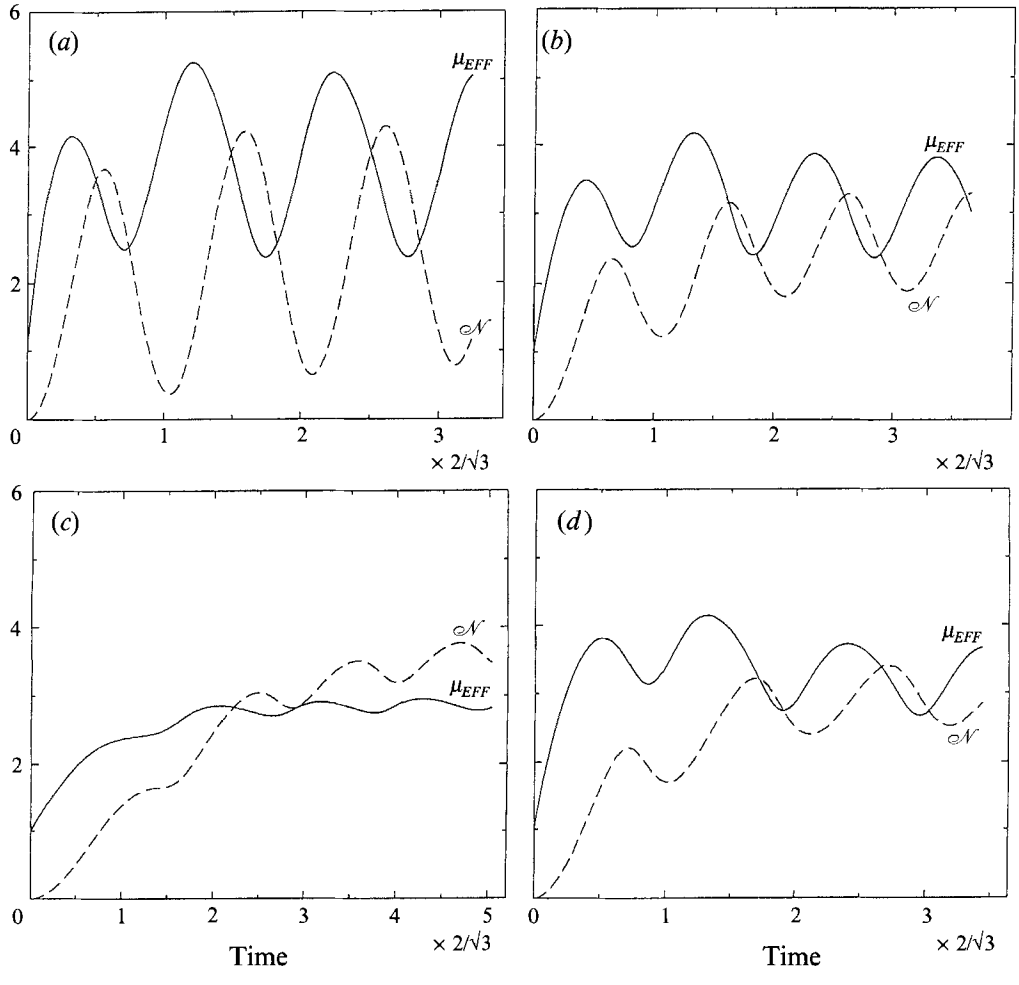

FIGURE 4. The evolution of the effective viscosity of the suspension μ_{EFF}, and normal stress difference $\mathcal{N}$, for $\lambda = 1$ and $\phi_d = 0.7216$ (*a*) $Ca_d = 0.02527$, (*b*) 0.04962, (*c*) 0.2527, for $N = 4$ and (*d*) 0.04962 for $N = 2$. Solid line for μ_{EFF}, dashed line for $\mathcal{N}$.

close to zero. As a secondary feature, we observe that at $Ca_d = 0.02527$ and 0.04962, μ_{EFF} overshoots at the second peak.

Comparing figure 4(*a*) to figure 2(*g*), we find that the oscillation of μ_{EFF} is nearly in phase with both the oscillation of the deformation parameter D and the inclination angle θ, indicating that elongated and inclined drops cause a higher viscous dissipation. Furthermore, the oscillation of $\mathcal{N}$ is nearly out of phase with the oscillation in θ. This is because that the non-circular shape of the drops introduces a global anisotropy, and the orientation of the drops serves to define the effective principal directions.

The overall dynamical behaviour of the suspensions may be characterized by the time-average values $\langle \mu_{EFF} \rangle$ and $\langle \mathcal{N} \rangle$ which are found by integrating μ_{EFF} and $\mathcal{N}$ over one cycle of the asymptotic motion at large times. In ZPI we found that the asymptotic value of the effective viscosity of single-file suspensions is a monotonically decreasing function of Ca, but as Ca is increased, $\mathcal{N}$ increases and reaches a maximum. Finally, as Ca tends to infinity, and the interface of the drops loses its dynamical significance, $\mathcal{N}$ decays to zero.

Ca_d	0.02527	0.04962	0.2527	∞
$\langle \mu_{EFF} \rangle$	3.7714	3.1381	2.8611	1
$\langle \mathcal{N} \rangle$	2.5244	2.5574	----	0

TABLE 1. A comparison of the time-average effective viscosity and normal stress difference for $N = 4$, $\phi_d = 0.7216$, $\lambda = 1$ at various Ca_d

Our computations indicate that ordered suspensions with multiple rows behave in a similar manner. Inspecting table 1 we find that as Ca_d is increased, $\langle \mu_{EFF} \rangle$ decreases, which indicates that the suspension is shear thinning, whereas $\langle \mathcal{N} \rangle$ is always positive, which indicates that the suspension exhibits some sort of elastic behaviour. These features have been observed in previous experiments on three-dimensional emulsions (Vadas *et al.* 1976; Han & King 1980) and are similar to those exhibited by polymeric solutions. In the extreme case $Ca_d = \infty$, $\langle \mathcal{N} \rangle$ vanishes because the interfaces are dynamically inactive.

Having described the behaviour of both the instantaneous and time-average viscometric functions, we turn to consider the contribution of viscous effects to the effective stress tensor by examining the functional dependence of $\langle \mu_{EFF} \rangle$ and $\langle \mathcal{N} \rangle$ on Ca_d. Assuming power-law relations of the form $\langle \mu_{EFF} \rangle \approx Ca_d^{\alpha-1}$ and $\langle \mathcal{N} \rangle \approx Ca_d^{\beta-1}$ at sufficiently small values of Ca_d, and using the data in table 1 for $Ca_d = 0.02527$ and 0.04962, we obtain the exponents $\alpha = 0.62$ and $\beta = 1.02$. Comparing these values with $\frac{2}{3} = 0.67$ and 1 predicted by the quasi-steady asymptotic analysis for foam of Reinelt & Kraynik (1990), we find good agreement.

In the model of Reinelt & Kraynik (1990), the effective stress tensor is computed using equation (3) of the present paper with the surface tension γ inside the integral. The viscous contribution is due to the excess surface tension associated with the viscous flow in the Plateau borders, and the scaling law emerge by applying the lubrication approximation (Mysels *et al.* 1959). In our formulation, viscous effects enter in an implicit manner by determining the instantaneous drop profiles. Because of these significant differences in physical behaviour, the above comparison serves only to demonstrate that the scaling laws are not to be expected to show significant variations in the limit as a concentrated emulsion becomes a foam.

4.2. *Effect of volume fraction*

To investigate the effect of volume fraction ϕ_d, we repeated the above computations with a reduced volume fraction $\phi_d = 0.388$ at the same values of the macroscopic capillary number Ca. Physically, these numerical experiments correspond to changing the drop size while maintaining the dimensions of the channel and the physical properties of the fluids constant. We observed behaviour similar to that described above but with lower mean values and amplitudes of oscillations of both μ_{EFF} and $\mathcal{N}$. For instance, for $Ca = 0.1$ we found $\langle \mu_{EFF} \rangle = 1.7821$ and $\langle \mathcal{N} \rangle = 0.1750$. It is interesting to note, in particular, that for $Ca = 0.1$ we obtained negative values for $\mathcal{N}$ during a small fraction of each temporal period; this emphasizes that the instantaneous and the time-average behaviour may show important differences. We find that the effective viscosity of a suspension increases with increasing the volume fraction of the suspended drops, in agreement with experimental observations and theoretical predictions for foam and concentrated emulsions (Bikerman 1973; Han & King 1980; Reinelt & Kraynik 1990).

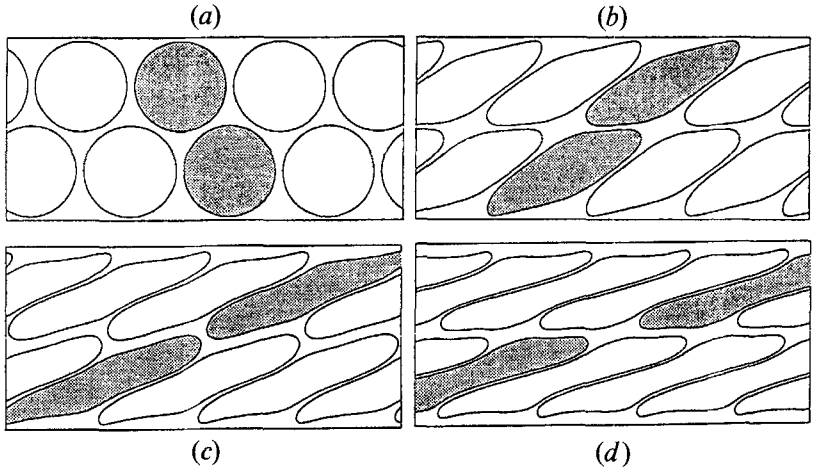

FIGURE 5. Drop profiles in a two-layer array with $\lambda = 1$, $Ca = 1.0$, $\phi_d = 0.7216$, at times (a) $t = 0$, (b) $3/\sqrt{3}$, (c) $5/\sqrt{3}$, (d) $7/\sqrt{3}$.

4.3. *Effect of number of rows*

We turn next to address the question of what the optimal way of dispersing the drops is in order to minimize the force on the walls required to sustain the motion of the fluid, subject to a given volume fraction and macroscopic shear rate. For this purpose, we consider the effect of number of rows N keeping the volume fraction at the constant value $\phi_d = 0.7216$, and carry out two simulations with $N = 2$ and $Ca = 0.1$, 1, corresponding to $Ca_d = 0.04962$, 0.4962.

For $Ca = 0.1$ or $Ca_d = 0.04962$ we observe that, after an initial transition period, the drops evolve in a periodic manner with period equal to $2/\sqrt{3}$ which is identical to that observed previously for $N = 4$. Comparing the viscometric functions shown in figure 4(*d*) to those for $N = 4$, $Ca = 0.1$ given in figure 4(*a*), we find lower mean values and smaller amplitudes of oscillation by a factor close to $\frac{2}{3}$. The first behaviour indicates that increasing the drop dispersivity raises the rate of viscous dissipation. The second behaviour may be understood by noting that the drop capillary number for $N = 2$, which is 0.04962, is higher than that for $N = 4$, which is 0.02527, but a higher capillary number implies reduced oscillations. We thus find that for a fixed volume fraction, increasing the number of rows causes the behaviour of the suspension to deviate more strongly from that exhibited by a Newtonian fluid. Comparing figure 4(*d*) with figure 4(*b*), we identify similar behaviour for μ_{EFF} and $\mathcal{N}$. These results suggest that the rheology of the suspension is best described in terms of the drop capillary number Ca_d rather than the macroscopic capillary number Ca.

For $Ca = 1$ or $Ca_d = 0.4962$ we find that the drops deform continuously without ever reaching either a stationary or an oscillatory state and the shape of the drops becomes convoluted, as illustrated in figure 5(*a–d*). Appreciable migration of the interfaces away from the wall are two distinguishing features of this motion. The nature of the asymptotic flow at large times could not be assessed with confidence, and two possible scenarios are that the drops develop a layered structure, or else break up to form four stable layers of smaller drops.

Reviewing the motion of the single file $N = 1$ studied in ZPI and those of the double and quadrable files $N = 2$, 4 considered here, we find that the first one is distinctly different, but the second and third exhibit similar features. These differences are attributed to the nature of drop interactions: for $N = 1$ drop interactions are mediated

by pairwise motions of side-by-side drops, whereas for $N > 1$ interactions between a drop and all of its surrounding neighbours in adjacent layers play dominant roles. Thus, studies of the single file have a limited capacity in describing the physics of the motion of general ordered suspensions and foams. But since the effects of the walls are confined to the first adjacent layers of drops, the motion of the two- and four-layered suspension provide accurate descriptions of the motion of an unbounded suspension that evolves under the action of a shear flow, and the convergence of the results with respect to the number of layers is fast.

4.4. *Effect of the viscosity ratio*

In ZPI we found that small drops with high viscosity $\lambda = 10$ arranged in a single file reach a steady state for any value of Ca. Large drops that occupy almost the whole of the clearance between the two walls, on the other hand, exhibit continuous deformation when Ca is sufficiently large. Our simulations indicate that multiple layers of high-viscosity drops filling a substantial portion of the clearance of the channel behave in a similar fashion, that is, they continue to elongate when Ca is sufficiently large. For instance, for $\lambda = 10$, $N = 4$, $\phi_d = 0.6063$, and $Ca = 1$, 10 we found no indication that the drops will ever reach an asymptotic oscillatory state.

In general, we find that the behaviour of the suspension is a weak function of λ, in contrast to the behaviour of solitary drops in a simple shear flow and drops in a single file where λ was seen to play a critical role in determining the asymptotic motion at large times. One explanation is that in multi-layered suspensions, the effects of surface tension and of the flow within the films separating adjacent drops are pronounced due to the increased interfacial area, whereas the viscous flow within the drops is of secondary importance.

4.5. *High volume fractions*

Thus far, we have considered suspensions whose volume fraction is lower than the critical volume fraction ϕ_d^* corresponding to maximum packing of circular drops. In the absence of intermolecular forces, stationary suspensions with higher volume fractions are not able to reach hydrostatic equilibrium without altering the topology of the initial state, and must evolve through film breakup and drop coalescence. Indeed, observations have shown that increasing ϕ_d from low values produces a continuous family of stable suspensions, but as ϕ_d approaches ϕ_d^* the suspensions tend to either self-destruct or invert so that the dispersed phase becomes the continuous phase and vice versa (Ostwald 1910; Princen 1979). Suspensions at higher volume fractions may be stabilized by the action of surface-active agents, and long-lived suspensions with volume fractions very close to 1 have been the subject of numerous experimental and theoretical studies (Kraynik 1988).

Our simulations in ZPI indicate that viscous forces in a suspension composed of a single file of large drops may prevent film breakup and stabilize the motion, at least for an extended period of time. To investigate this possibility for a suspension with multiple layers, we consider the evolution of a hexagonal array of hexagonal drops illustrated in figure 6(*a*). Each drop in a middle row is contained within a hexagonal cell with side length b, and its corners are rounded off to form circular arcs of radius r. At small film thicknesses, r depends on b and the volume fraction through the relation $r = \sqrt{3}b(1-\phi_d)^{\frac{1}{2}}/[(1/2-\pi/\sqrt{3})^{\frac{1}{2}}]$. The width of a drop is given by $w = \sqrt{3}b$, and b may be computed from the number of files N and the area fraction ϕ_d (Princen 1985, Appendix 1). The boundaries of the drops that are adjacent to the walls are pentagons with side length w, and the radii of the two wall corners of the pentagonal drop are equal to those of the rest of the corners.

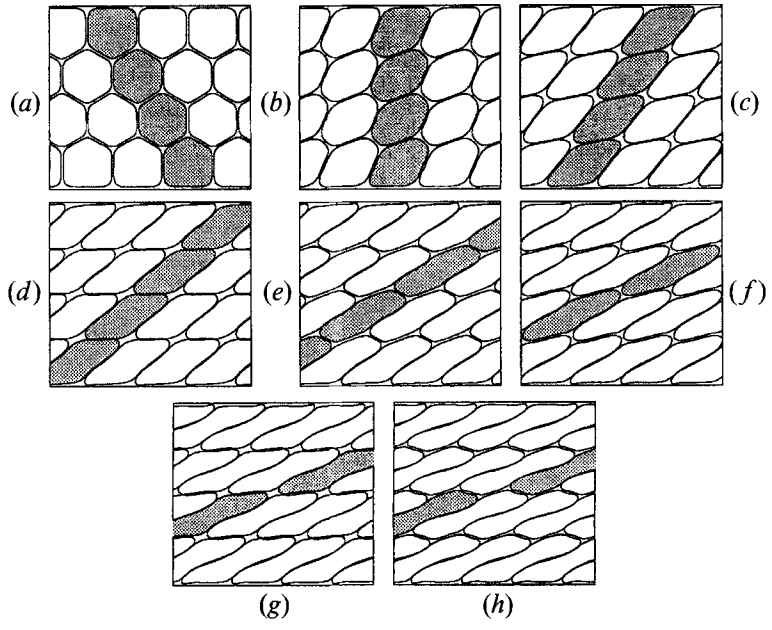

FIGURE 6. Profiles of initially hexagonal drops in a hexagonal lattice with $\lambda = 1$, $Ca = 1.0$, $\phi_d = 0.8974$, at times: (*a*) $t = 0$, (*b*) $1/\sqrt{3}$, (*c*) $2/\sqrt{3}$, (*d*) $3/\sqrt{3}$, (*e*) $4/\sqrt{3}$, (*f*) $5/\sqrt{3}$, (*g*) $6/\sqrt{3}$, (*h*) $7/\sqrt{3}$.

In figure 6(*a–h*), we present several stages in the evolution of a suspension of hexagonal drops with $N = 4$, $\phi_d = 0.8974$, $\epsilon = 0.05$, $\lambda = 1$, and $Ca = 1$. Switching of neighbouring drops and 'hopping' or 'T1' occur in a more complicated way than those for idealized foams discussed by previous authors (Kraynik 1988; Reinelt & Kraynik 1990). Clearly, this difference is due to the effects of the fluid flow within the thin films, at the Plateau borders, and inside the drops. Although the concentrated suspension appears to perform a global periodic motion, examining the detailed shape of the interfaces shows that viscous forces that might have acted to prevent film collapse, are not strong enough to inhibit squeezing motions. As a result, the surfaces of two adjacent drops overlap, meaning that the thin films separating adjacent drops tend to collapse at a finite time bringing the numerical simulations to an end. After film breakup, the drops will coalesce, small islands of suspending fluid will develop, and the suspension will invert. This behaviour demonstrates explicitly the critical importance of intermolecular forces and surface-active agents on the stability of a foam. Computations with $Ca = 0.2$, and 0.1 revealed similar behaviour, but with an earlier time of film breakup and drop coalescence.

5. Random suspensions

In the second stage of our numerical investigations we perform two dynamic simulations (hereafter referred as random 1 and 2, respectively) of a disordered suspension beginning with two different initial configurations but identical flow conditions. At the initial instant, 12 circular drops are placed randomly within each periodic cell of dimensions 4 by 2 which is bounded from above and below by the two walls. This is the maximum number that could be accommodated with sufficient accuracy using the available computational resources. Throughout a simulation, the

average number of marker points per drop is roughly 40, which is large enough to warrant a sufficiently accurate representation of the interfaces and solutions of the integral equations.

The initial positions of the drop centres were determined by a random-number generator. The radius of each drop was set equal to 0.25 yielding a volume fraction of 0.2945 which is close to the areal fraction 0.30 corresponding to the monolayered simulations of rigid spheres presented by Durlofsky & Brady (1989). Furthermore, we set $\lambda = 1$ for computational convenience, and $Ca = 1$, or $Ca_d = 0.25$ in order to prevent drop breakup but maintain an appreciable degree of particle deformability. Both random 1 and 2 were carried out until $t = 22.6$, which was found to be long enough for the main features of the motion to emerge and the computation of time averages to be meaningful.

5.1. *Drop motions and the structure of the flow*

In figures 7(*a–j*) and 8(*a–e*) we present a sequence of instantaneous drop profiles from the beginning to the end of the simulation for random 1 and 2, respectively. One may observe a variety of motions including formation of clusters of two, three, or more interacting drops, and pairing between the clusters themselves. These motions have a strong impact on the elongation and orientation of the individual drops, and we observe highly elongated shapes, sigmoidal shapes, as well as dimpled shapes during collisions. A motion-picture video of both of the simulations clearly illustrated that this behaviour is a consequence of pairing, tripling, and higher-order interactions, involving head-on interceptions, orbiting motions, and bypassing. In a typical scenario, two drops approach each other, usually side by side, a thin liquid film of ambient fluid is trapped between the interfaces, and the film develops a dimple under the action of local pressure fields. The drops move normal as well as tangential to each other, and eventually slide over and bypass each other, relaxing to a smooth shape until the next interception.

Although there are circumstances where two drops are extremely close to each other, as can be seen for drops 9 and 11 in figure 7(*e–h*) and drops 8 and 9 in figure 8(*e*), strong adherence and coalescence were not observed. Furthermore, at the capillary number $Ca_d = 0.25$, the shearing motion of the fluid is not strong enough to cause excessive drop distortion and fragmentation, and the drops manage to maintain a compact shape throughout the simulation.

To illustrate the motion of the individual drops in more detail, in figure 9(*a*) we present the time evolution of the lateral position of the drop centres for random 1. We observe that drops 1 and 12, which are initially closest to the walls, migrate away from the walls, whereas drops 4 and 10, which are initially located roughly halfway between the walls and the centreline, migrate toward the walls. Drop 5 migrates from the upper half to the lower half of the channel, whereas drop 8 migrates from the lower half to the upper half of the channel. Drop 3 wiggles as it moves towards the centreline of the channel, and drops 6 and 9 perform upward and downward net motions. For random 2 we observe similar scenaria of drop motions. Figure 9(*a*) clearly suggests that there is a systematic migration of the drops away from the two walls.

To paint a coherent picture of collective drop motions, in figure 9(*b*) we plot the trajectories of the centre of all drops initially residing within one periodic cell for random 1. One group of drops, including drops 5, 7 and 8 in random 1 and drops 5 and 7 in random 2, remain within the original cell, but another group leave the cell and are convected upstream or downstream far from their initial position, with the exceptions of drops 8 and 9 in random 2 that are first convected downstream then turn

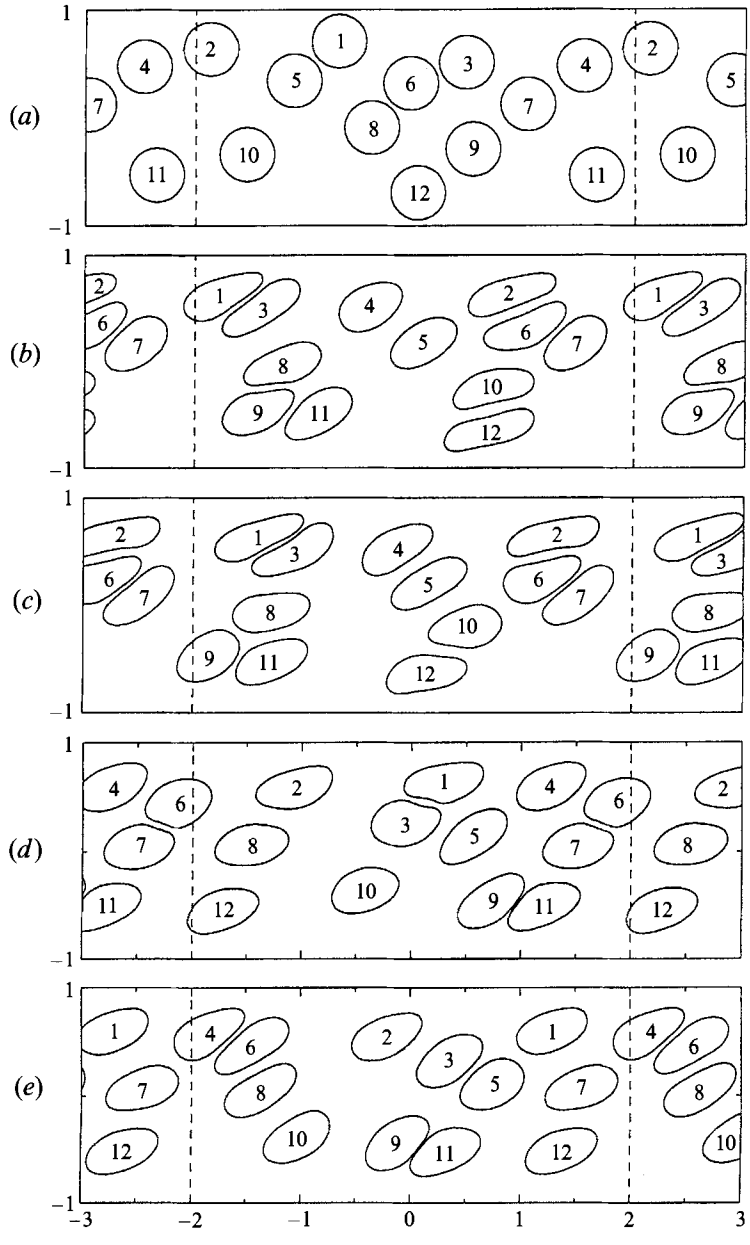

FIGURE 7. For caption see facing page.

around. It is interesting, in particular, to note that erratic motion of drops in the first groups, especially that of drop 7 in random 1 and of drop 5 in random 2. There are considerable changes in the transverse position of drops in the second group due to particle interceptions.

In order to detect preferential drop migrations, it is useful to consider the density distribution of the centres of the drops across the channel. For this purpose, following Durlofsky & Brady (1989), we divide the central region of the channel ($-0.75 < y < 0.75$) into 15 horizontal zones, calculate the number of drop centres

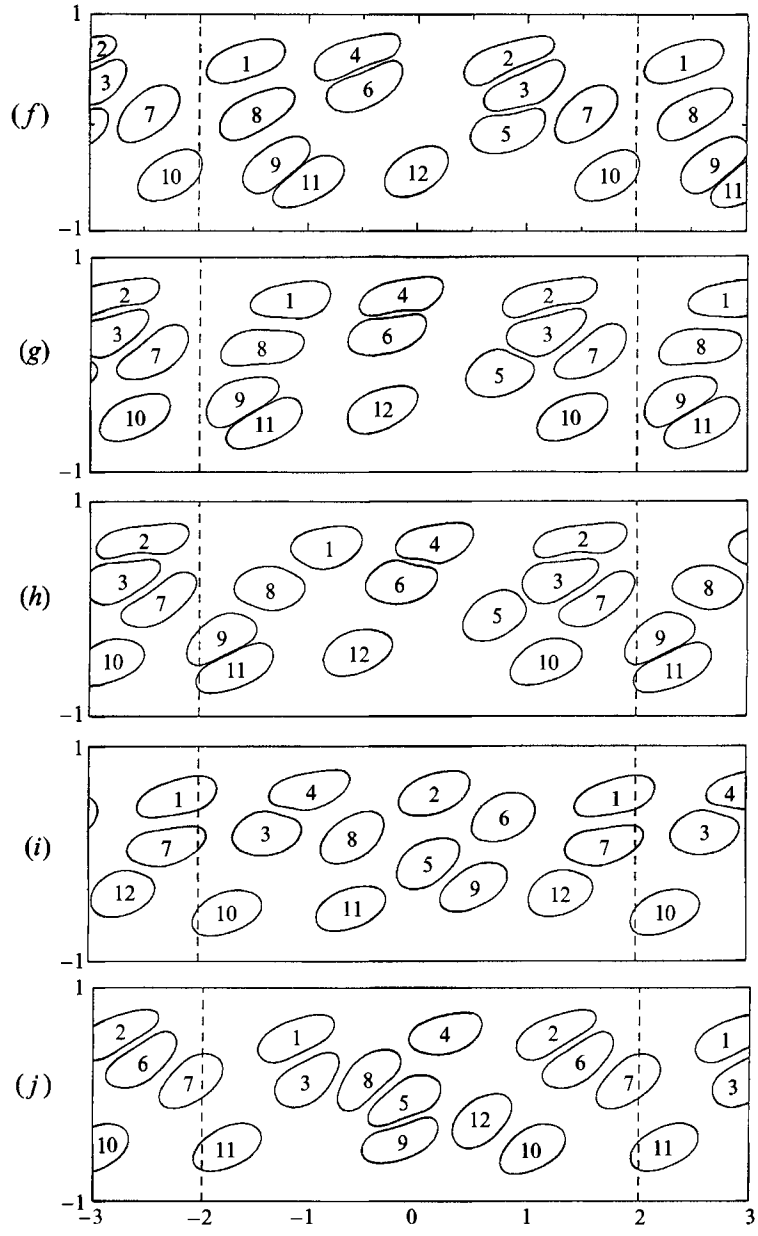

FIGURE 7. The evolution of a random suspension of 12 drops with $\lambda = 1$, $Ca_a = 0.25$, $a = 0.25$, $\phi_a = 0.2945$ (random 1) at times: (*a*) $t = 0$, (*b*) 4.875, (*c*) 5.645, (*d*) 8.730, (*e*) 10.511, (*f*) 13.084, (*g*) 13.876, (*h*) 14.404, (*i*) 20.168, (*j*) 22.608.

within each zone, and normalize it by the total number of drops, i.e. 12, to obtain the instantaneous density distribution. Finally, we compute the time-average density distribution within each zone over the time period $2.0 < t < 22.6$, having excluded the initial transient period $0 < t < 2$ (see figure 10). The results of this computation, shown in figure 9(*c*, *d*), reveal high peaks near the two walls and large fluctuations around the centreline. These features are familiar from the dynamic simulations of random suspensions of rigid spheres of Durlofsky & Brady (1989). In figure 9(*c*, *d*) we also

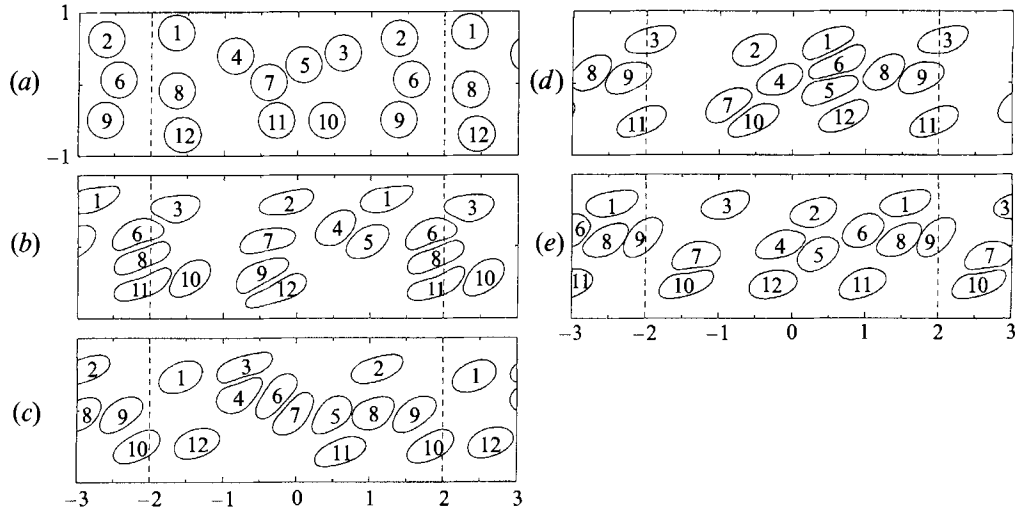

FIGURE 8. The evolution of a random suspension of 12 drops with $\lambda = 1$, $Ca_d = 0.25$, $a = 0.25$, $\phi_d = 0.2945$ (random 2) at times: (*a*) $t = 0$, (*b*) 4.22, (*c*) 14.32, (*d*) 19.68, (*e*) 21.76.

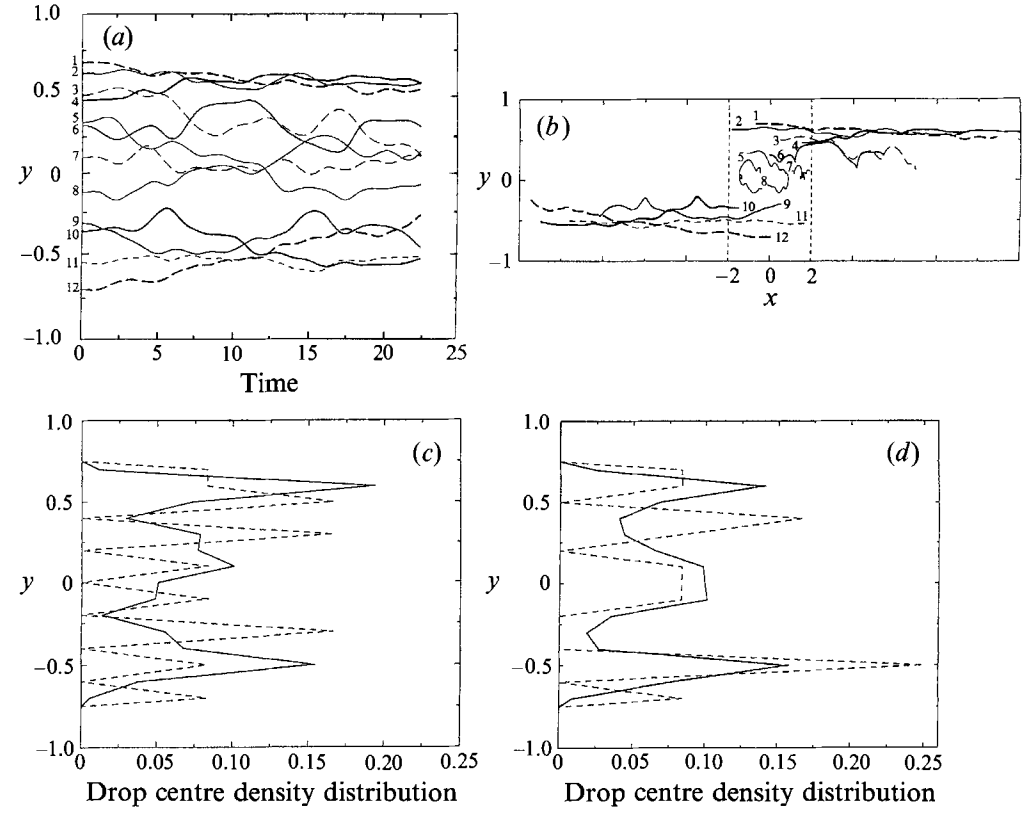

FIGURE 9. Features of the motion of a random suspension: (*a*) the evolution of the lateral position of the drop centres; (*b*) drop centre trajectories; (*c*, *d*) the density distribution of drop centres across the channel; the dashed line shows the distribution at the initial instant. (*a*, *b*, *c*) are for random 1 and (*d*) for random 2.

show the density distribution of the initial state, which may be used as a reference to demonstrate global drop migrations.

Although the general features of the number-density distribution of liquid drops are similar to those of rigid particles, some important differences are identified. First, the wall peaks for liquid drops are located farther from the walls than those for spherical particles; this is clear evidence of enhanced particle migration due to deformability. Furthermore, in the case of liquid drops, the intensity of the wall peaks is significantly higher than the amplitude of the fluctuations near the centreline, in contrast to the case of spherical particles where the two have comparable magnitudes. This difference may be attributed to the moderate number of particles used in our simulations, which is 12 at a volume fraction of 0.2945, compared to 49 particles at an areal fraction of 0.3 used by Durlofsky & Brady (1989). Unfortunately, the moderate number of particles used in our simulation does not allow us to make any definitive conclusions regarding the statistics of the motion.

To complete the description of the motion of the individual drops, we consider the evolution of the deformation parameter D and orientation angle θ. Our results reveal an initial monotonic growth of D from the initial value of 0, and a monotonic decrease of θ from the initial value of $\pi/4$, for all drops up to $t = 2$, and strong subsequent fluctuations. It is interesting to note that the orientation angle θ of a couple of drops in both simulations becomes negative over a short period of the evolution owing to orbiting motions. Time-average values of D for each drop ranged between 0.3121 for drop 12 and 0.4405 for drop 2 in random 1 and between 0.3069 for drop 9 to 0.3822 for drop 1 in random 2, and time-average values of θ ranged between 0.1044π for drop 1 and 0.1713π for drop 9 in random 1 and between 0.1149π for drop 1 and 0.1768π for drop 8 in random 2. More extensive data on this statistics are presented in Zhou (1993).

Drawing instantaneous velocity profiles at various locations across the channels showed appreciable deviations from the linear profile that would prevail in the absence of the drops, due to the local motions associated with the presence of the drops (Zhou 1993).

Overall, comparing the statistics of the motion of the two random suspensions, we find basically identical behaviour which indicates that the initial configuration loses its significance after a certain period of evolution.

5.2. *Effective stresses*

In figure 10(*a*, *b*) we plot the evolution of the effective viscosity μ_{EFF} and normal stress difference $\mathcal{N}$, and observe an initial transient period up to $t = 2$, and subsequent mild fluctuations around the well-defined mean values $\langle \mu_{EFF} \rangle = 1.456$ and $\langle \mathcal{N} \rangle = 0.773$ for random 1 and $\langle \mu_{EFF} \rangle = 1.435$ and $\langle \mathcal{N} \rangle = 0.713$ for random 2. The fluctuations of μ_{EFF} are significantly weaker than those of $\mathcal{N}$. The effect of the microstructure on the effective stresses may be illustrated by examining the instantaneous profiles shown in figures 7(*a–j*) and 8(*a–e*) with reference to figure 10(*a*, *b*). We observe that at the times corresponding to figures 7(*b*, *f*, *j*) and 8(*d*), μ_{EFF} reaches local maxima, whereas at the times corresponding to figures 7(*d*, *h*, *i*) and 8(*e*), μ_{EFF} reaches local minima. In the first case, the microstructure is characterized by evolving clusters with elongated drops; in the second case, the drops are distributed in a relatively uniform manner throughout the channel. The normal stress difference $\mathcal{N}$ reaches local maxima in figures 7(*c*, *g*) and 8(*b*), where the drops are oriented along the channel, and local minima in figures 7(*e*, *j*) and 8(*c*), where the drops are oriented in the principal direction of the shearing flow, i.e. at 45° with respect to the channel.

Our previous experience with ordered suspensions suggests that the effective stresses

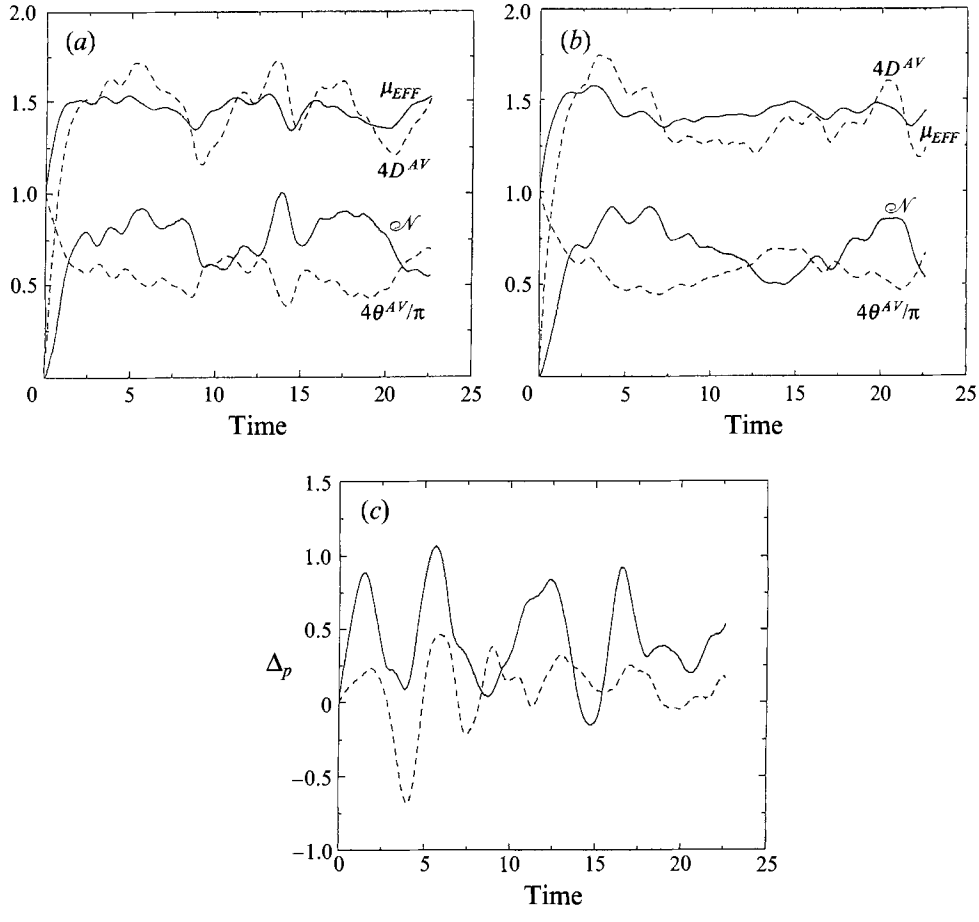

FIGURE 10. The evolution of the shear effective viscosity μ_{EFF}, normal stress difference $\mathcal{N}$, mean drop deformation parameter D^{AV}, and mean orientation angle θ^{AV}, averaged over all drops for (*a*) random 1, (*b*) random 2; (*c*) the evolution of the pressure drop Δp over one period, solid line is for random 1, dashed line for random 2.

in the suspension may correlate with the global geometrical state of the drops. To illustrate the dynamics of the latter, in figure 10(*a*, *b*) we plot the evolution of the mean values of D and θ averaged over all drops, denoted by D^{AV} and θ^{AV}, and observe strong fluctuations around the mean values of 0.3697 and 0.1361π for random 1 and of 0.3504 and 0.1403π for random 2, respectively, at large times. Comparing the four curves in figure 10(*a*, *b*) it is observed that the oscillations of μ_{EFF} are nearly in phase with those of D^{AV} and θ^{AV} whereas those of $\mathcal{N}$ are nearly out of phase with those of θ^{AV}. This intriguing behaviour, which is identical to that observed previously for ordered suspensions, suggests there exists a correlation between particle shapes and effective stresses, independently of the ordered or random structure of the suspension, at least at moderate volume fractions.

Durlofsky & Brady (1989) found that μ_{EFF} reaches a maximum when clusters of particles are oriented at an angle close to 45° with respect to the walls, and a minimum when they are aligned in the direction of the walls. We find that μ_{EFF} reaches a maximum when the drops are inclined at a maximum angle with respect to the walls. Unfortunately, we are not able to assess the effect of orientation of the clusters

	$N = 2$	$N = 3$	Random 1	Random 2
$\langle \mu_{EFF} \rangle$	1.324	1.375	1.456	1.435
$\langle \mathcal{N} \rangle$	0.468	0.726	0.773	0.713

TABLE 2. A comparison of the time-average effective viscosity and normal stress difference for ordered suspensions with $N = 2$, 3, and the random suspensions with $\lambda = 1$, $Ca_d = 0.25$, $a = 0.25$ and $\phi_d = 0.2945$

themselves owing to the small number of particles involved in our simulation. The synergy or competition between drop inclination and cluster orientation is likely to introduce some novel types of behaviour whose analysis requires further investigations.

Comparing the effective shear viscosity of a random suspension of drops to that of a random suspension of rigid spheres (Durlofsky & Brady 1989), we find that the former is lower in magnitude, and exhibits noticeably weaker fluctuations. The first feature may be understood by noting that, in the case of liquid drops, with $\lambda = 1$, the excess dissipation is due exclusively to motions induced by surface tension and thus it decreases as the capillary number is increased. The second feature might have been attributed to differences in the number of suspended particles used in the two simulations, 12 versus 49 for virtually identical areal fractions, but it has been shown that increasing the number of particles diminishes the amplitude of the fluctuations (Blanc *et al.* 1983). Thus, it is more likely that this difference is due to more fundamental physical reasons. It is known, for instance, that the near-contract interaction of drops is fundamentally different from that of rigid particles, for in the second case, strong lubrication forces assume a dominant role, and particle interactions cause stronger oscillations in the effective stresses (Davis, Schonberg & Rallison 1989). Furthermore, wall–particle interactions, and associated contributions to the effective stresses are weaker for drops than those for rigid particles owing to more pronounced particle migrations away from the walls.

To demonstrate the consequence of ordering the microstructure, in table 2 we compare the time-average values $\langle \mu_{EFF} \rangle$ and $\langle \mathcal{N} \rangle$ for the random suspensions to those for ordered suspensions where drops with the same size ($a = 0.25$) and volume fraction ($\phi_d = 0.2945$) are placed homogeneously in two and three rows. We note that the random suspensions have a higher shear viscosity and normal stress difference, which may be attributed to stronger interactions among intercepting drops and accompanying increased rates of viscous dissipation. We may conclude that at $\phi_d = 0.2945$, particle interceptions and near-contact particle interactions play a dominant role in determining the rheology of the suspension. It is not certain, however, that this trend will remain at higher volume fractions, for the energy dissipation in the films surrounding the drops in an ordered suspension might be larger than that due to the particle interceptions occurring in a disordered system.

In figure 10(*c*) we show the evolution of the pressure drop over one periodic cell, Δp, and observe noticeable fluctuations. The overall magnitude of Δp in random 1 is somewhat larger than that in random 2, suggesting that Δp is sensitive to the geometry of the microstructure. It is interesting to note that Δp may take positive or negative values, and the bias in random 1 is at positive whereas that in random 2 is at negative values. Δp is straightforward to measure in an experimental apparatus, and our results advocate its use for probing the instantaneous state of the motion.

The authors wish to thank Dr A. M. Kraynik, and Professors J. D. Goddard, W. R.

Schowalter and R. Skalak for useful discussions and helpful comments. This work is supported by the National Science Foundation, Grants CTS-9020728 and CTS-9216176. Computing time was granted by the San Diego Supercomputer Center and the Division of Engineering of UCSD.

REFERENCES

ADLER, P. M. & BRENNER, H. 1985 Spatially periodic suspensions of convex particles in linear shear flows. I. Description and kinematics. *Intl J. Multiphase Flow* **11**, 361–385.

BATCHELOR, G. K. 1970 The stress system in a suspension of force-free particles. *J. Fluid Mech.* **41**, 545–570.

BIKERMAN, J. J. 1973 *Foams*. Springer.

BLANC, R., BELZONS, M., CAMOIN, C. & BOUILLOT, J. L. 1983 Cluster statistics in bidimensional suspension: comparison with percolation. *Rheol. Acta* **22**, 505–511.

BRADY, J. F. & BOSSIS, G. 1988 Stokesian dynamics. *Ann. Rev. Fluid Mech.* **20**, 111–157.

COX, R. G. & MASON, S. G. 1971 Suspended particles in fluid flow through tubes. *Ann. Rev. Fluid Mech.* **5**, 291–316.

DAVIS, R. H., SCHONBERG, J. A. & RALLISON, J. M. 1989 The lubrication force between two viscous drops. *Phys. Fluids* A **1**, 77–81.

DURLOFSKY, L. J. & BRADY, J. K. 1989 Dynamic simulation of bounded suspensions of hydrodynamically interacting spheres. *J. Fluid Mech.* **200**, 39–67.

FRANKEL, N. A. & ACRIVOS, A. 1970 The constitutive equation for a dilute emulsion. *J. Fluid Mech.* **44**, 65–78.

GAUTHIER, F. J., GOLDSMITH, H. L. & MASON, S. G. 1972 Flow of suspensions through tubes–X Liquid drops as models of erythrocytes. *Biorheology* **9**, 205–224.

GODDARD, J. D. 1986 Microstructural origins of continuum stress fields – A brief history and some unresolved issues. In *Recent Developments in Structured Continua* (ed. D. Dekee & P. N. Kaloni). Pitman Research Notes in Mathematics, No. 143, Chap. 6, pp. 179–208. Longman/J. Wiley.

HAN, C. D. & KING, R. G. 1980 Measurement of the rheological properties of concentrated emulsions. *J. Rheol.* **24**, 213–237.

KENNEDY, M. R., POZRIKIDIS, C. & SKALAK, R. 1993 Motion and deformation of liquid drops and the rheology of dilute emulsions in simple shear flow. *Computers Fluids* (in press).

KHAN, S. A. & ARMSTRONG, R. C. 1986 Rheology of foams: I. Theory for dry foams. *J. Non-Newtonian Fluid Mech.* **22**, 1–22.

KHAN, S. A. & ARMSTRONG, R. C. 1987 Rheology of foams: II. Effects of polydispersity and liquid viscosity for foams having gas fraction approaching unity. *J. Non-Newtonian Fluid Mech.* **25**, 61–92.

KRAYNIK, A. M. 1988 Foam flow. *Ann. Rev. Fluid Mech.* **20**, 325–357.

KRAYNIK, A. M. & HANSEN, M. G. 1986 Foam and emulsion rheology: a quasistatic model for large deformations of spatially periodic cells. *J. Rheol.* **30**, 409–439.

KRAYNIK, A. M. & HANSEN, M. G. 1987 Foam rheology: a model of viscous phenomena. *J. Rheol.* **31**, 175–205.

KRAYNIK, A. M. & REINELT, D. A. 1992 Simple shearing flow of a 3D foam. In *Theoretical and Applied Rheology* (ed. P. Moldenaers & R. Keunings), pp. 675–677. Elsevier.

KRAYNIK, A. M. & REINELT, D. A. & PRINCEN, H. M. 1991 The nonlinear elastic behaviour of polydisperse hexagonal foams and concentrated emulsions. *J. Rheol.* **35**, 1235–1253.

MASLIYAH, J. H. & VEN, T. G. M. VAN DE. 1986 A two-dimensional model of the flow of ordered suspensions of rods. *Intl J. Multiphase Flow* **12**, 791–806.

MYSELS, K. J., SHINODA, K. & FRANKEL, S. 1959 *Soap Films: Studies of Their Thinning*. Pergamon.

NOTT, P. R. & BRADY, J. F. 1991 Dynamic simulation of pressure driven suspension flow. *Proc. DOE/NSF Workshop on Particulate Flows, Worcester, MA.*

OSTWALD, W. VON. 1910 Beiträge zur Kenntnis der Emulsionen. *Kolloid Z.* **6**, 103–109.

POZRIKIDIS, C. 1992 *Boundary Integral and Singularity Methods for Linearized Viscous Flow*. Cambridge University Press.

POZRIKIDIS, C. 1993 On the transient motion of ordered suspensions of liquid drops. *J. Fluid Mech.* **246**, 301–320.

PRINCEN, H. M. 1979 Highly concentrated emulsions. I. Cylindrical systems. *J. Colloid Interface Sci.* **71**, 55–66.

PRINCEN, H. M. 1983 Rheology of foams and highly concentrated emulsions I. Elastic properties and yield stress of a cylindrical model system. *J. Colloid Interface Sci.* **91**, 60–75.

PRINCEN, H. M. 1985 Rheology of foams and highly concentrated emulsions II. Experimental study of the yield stress and wall effects for concentrated oil-in-water emulsions. *J. Colloid Interface Sci.* **105**, 150–171.

RALLISON, J. M. & ACRIVOS, A. 1978 A numerical study of the deformation and burst of a viscous drop in an extensional flow. *J. Fluid Mech.* **89**, 191–200.

REINELT, D. A. & KRAYNIK, A. M. 1989 Viscous effects in the rheology of foams and concentrated emulsions. *J. Colloid Interface Sci.* **132**, 491–503.

REINELT, D. A. & KRAYNIK, A. M. 1990 On the shearing flow of foams and concentrated emulsions. *J. Fluid Mech.* **215**, 431–455.

REINELT, D. A. & KRAYNIK, A. M. 1992 Large elastic deformations of three-dimensional foams and highly concentrated emulsions. *J. Colloid Interface Sci.* (submitted).

REVAY, J. M. & HIGDON, J. J. L. 1992 Numerical simulation of polydisperse sedimentation: equal-sized spheres. *J. Fluid Mech.* **243**, 15–32.

ROSENKILDE, C. E. 1967 Surface-energy tensors. *J. Math. Phys.* **8**, 84–88.

SCHOWALTER, W. R., CHAFFEY, C. E. & BRENNER, H. 1968 Rheological behaviour of a dilute emulsion. *J. Colloid Interface Sci.* **26**, 152–160.

SCHWARTZ, L. W. & PRINCEN, H. M. 1987 A theory of extensional viscosity for flowing foams and concentrated emulsions. *J. Colloid Interface Sci.* **118**, 201–211.

SKALAK, R., ÖZKAYA, N. & SKALAK, T. C. 1989 Biofluid mechanics. *Ann. Rev. Fluid Mech.* **21**, 167–204.

SMART, J. R. & LEIGHTON, D. T. 1991 Measurement of the drift of a droplet due to the presence of a plane. *Phys. Fluids* A **3**, 21–28.

TAYLOR, G. I. 1932 The viscosity of a fluid containing small drops of another fluid. *Proc. R. Soc. Lond.* A **138**, 41–48.

TAYLOR, G. I. 1934 The formation of emulsions in definable fields of flow. *Proc. R. Soc. Lond* A **146**, 501–523.

VADAS, E. B., GOLDSMITH, H. L. & MASON, S. G. 1976 The microrheology of colloidal dispersions. III. Concentrated emulsions. *Trans. Soc. Rheol.* **20**, 373–407.

ZHOU, H. 1993 Numerical studies of the flow of suspensions of two-dimensional liquid drops in channels. Doctoral dissertation, University of California at San Diego.

ZHOU, H. & POZRIKIDIS, C. 1993 The flow of suspensions in channels: single files of drops. *Phys. Fluids* A **5**, 311–324 (referred to herein as ZPI).